Modelling the synergistic effect of bacteriophage and antibiotics on bacteria: killers and drivers of resistance evolution

Quentin J. Leclerc [1,2,3]*, Jodi A. Lindsay [3], Gwenan M. Knight [1,2]

[1] Centre for Mathematical Modelling of Infectious Diseases, Department of Infectious Disease Epidemiology, Faculty of Epidemiology & Population Health, London School of Hygiene & Tropical Medicine, UK

[2] Antimicrobial Resistance Centre, London School of Hygiene and Tropical Medicine, UK

[3] Institute for Infection & Immunity, St George's University of London, UK

* corresponding author: quentin.leclerc@lshtm.ac.uk (QJL)

ABSTRACT

Bacteriophage (phage) are bacterial predators that can also spread antimicrobial resistance (AMR) genes between bacteria by generalised transduction. Phage are often present alongside antibiotics in the environment, yet evidence of their joint killing effect on bacteria is conflicted, and the dynamics of transduction in such systems are unknown. Here, we combine *in vitro* data and mathematical modelling to identify conditions where phage and antibiotics act in synergy to remove bacteria or drive AMR evolution.

We adapt a published model of phage-bacteria dynamics, including transduction, to add the pharmacodynamics of erythromycin and tetracycline, parameterised from new *in vitro* data. We simulate a system where two strains of *Staphylococcus aureus* are present at stationary phase, each carrying either an erythromycin or tetracycline resistance gene, and where multidrug-resistant bacteria can be generated by transduction only. We determine rates of bacterial clearance and multidrug-resistant bacteria appearance, when either or both antibiotics and phage are present at varying timings and concentrations.

Although phage and antibiotics act in synergy to kill bacteria, by reducing bacterial growth antibiotics reduce phage production. A low concentration of phage introduced shortly after antibiotics fails to replicate and exert a strong killing pressure on bacteria, instead generating multidrug-resistant bacteria by transduction which are then selected for by the antibiotics. Multidrug-resistant bacteria numbers were highest when antibiotics and phage were introduced simultaneously.

The interaction between phage and antibiotics leads to a trade-off between a slower clearing rate of bacteria (if antibiotics are added before phage), and a higher risk of multidrug-resistance evolution (if phage are added before antibiotics), exacerbated by low concentrations of phage or antibiotics. Our results form hypotheses to guide future experimental and clinical work on the impact of phage on

AMR evolution, notably for studies of phage therapy which should investigate varying timings and concentrations of phage and antibiotics.

AUTHOR SUMMARY

Bacteriophage ("phage") are viruses that can infect and kill bacteria, but also natural drivers of antimicrobial resistance (AMR) evolution by transduction, when they carry non-phage DNA between bacteria, including AMR genes. Phage are often present alongside antibiotics in the environment and in humans, yet the joint dynamics of phage, antibiotics, and bacteria are unclear. Using laboratory work and mathematical modelling, we show for the first time that depending on timing and concentration, phage and antibiotics can either work together to kill bacteria faster, or phage can generate multidrug-resistant bacteria by transduction which are then selected for by antibiotics. This may be particularly important in the context of phage therapy, where phage are used to treat bacterial infections, often alongside antibiotics. Our conclusions highlight the urgent need for clinical and laboratory work to quantify the currently unknown contribution of phage to AMR evolution in humans. Otherwise, we may be missing opportunities to reduce the global public health burden of AMR.

INTRODUCTION

Bacteriophage (phage) are major bacterial predators and the most common organisms on the planet [1]. Phage are often present alongside antibiotics, naturally or in the context of antibacterial treatment [2–4], yet reports on their combined effect on bacteria are conflicting. Some previous studies showed that phage and antibiotics work synergistically to clear bacteria [5–8], while others have demonstrated that antibiotics reduce phage production [9,10]. This interaction has been extensively studied in biofilms to show that adding phage to disrupt the biofilm before adding antibiotics leads to the greatest synergistic killing [11–13]. However, whilst there is some work suggesting a similar timing-dependent synergistic killing effect on planktonic bacteria [6–8], this evidence is limited as only a few timings and concentrations of phage and antibiotics have been explored experimentally. This is further complicated by the fact that phage are also major drivers of bacterial evolution via horizontal gene transfer by transduction [14,15], which can notably contribute to antimicrobial resistance (AMR) spread [16,17]. If multidrug-resistant bacteria are generated by transduction, antibiotics present in the same environment may act as a synergistic selective pressure to increase their prevalence, yet to our knowledge the dynamics of transduction have not yet been investigated in such systems [18].

There are two types of transduction: specialised and generalised [19,20]. Specialised transduction occurs when a prophage sometimes picks up adjacent bacterial DNA upon excision from the bacterial chromosome, at the end of the lysogenic cycle. We also note lateral transduction as an important variation of specialised transduction, where phage packaging occurs before the prophage is excised from the bacterial chromosome, leading to transfer of DNA located further downstream of the prophage [21]. On the other hand, generalised transduction occurs during phage replication, when random non-phage DNA is packaged instead of phage DNA in a new phage particle. The resulting transducing phage is released upon bacterial lysis, and injects this DNA in another bacterium. Generalised transduction is likely the most important type of transduction in the context of AMR, as

77 it can lead to the horizontal transfer of any genetic material contained in a bacterium (including
78 plasmids, major vectors of AMR genes) [14].

79 A major bacterial pathogen often exposed to phage is *Staphylococcus aureus*, which at any given time
80 is colonising approximately 20% of humans [22]. Previous work suggests that all *S. aureus* carry
81 integrated prophage [23], and at least 50% of individuals colonised by *S. aureus* also carry free phage
82 capable of generalised transduction [24], the main mechanism of horizontal gene transfer for *S. aureus*
83 [23]. This is particularly relevant for methicillin-resistant *S. aureus* (MRSA), a group of *S. aureus* present
84 in both the ESKAPE list and the World Health Organization priority list of antibiotic-resistant bacteria
85 due to its large clinical burden [25–27]. *In vitro*, the generation rate of generalised transducing MRSA
86 phage carrying an AMR gene has been estimated to be approximately one per 10^8 new phage
87 produced, sufficient to consistently generate bacteria resistant to multiple antibiotics in less than 24h
88 [28], and *in vivo* transduction rates are likely to be even higher [29].

89 Understanding the dynamics of bacteria, antibiotics, phage and transduction is especially important
90 in the context of phage therapy, which aims to use phage as antibacterial agents, generally in
91 combination with antibiotics [4]. Phage therapy is currently investigated as a solution to counter the
92 threat of AMR, with ongoing clinical trials against MRSA infection [6,30–34]. Phage therapy guidelines
93 recommend that only phage with a limited ability to perform transduction should be used [19,35,36],
94 yet to our knowledge there is currently no technique to prevent phage from accomplishing generalised
95 transduction, which is fundamentally a mispackaging and thus a biological error similar to a mutation.
96 Hence, as previous reviews have highlighted, it is essential to explore the importance of this
97 mechanism, and identify conditions under which it could affect the outcome of therapy and lead to
98 multidrug-resistance evolution [18,35–37].

99 In this study, we aim to investigate the potential combined effect of antibiotics and phage capable of
100 generalised transduction on bacteria. Making conclusions about this multidimensional chequerboard
101 space of potential combinations and timings is difficult when using data from time-consuming, single-

scenario, *in vitro* experiments. Instead, we generate hypotheses to guide future experimental work by simulating these conditions. We extend a previously published mathematical model of only phage-bacteria dynamics, including generalised transduction, to newly incorporate the effect of antibiotics on bacteria [28]. This model is parameterised using *in vitro* data from the same environment and set of conditions as when it was originally developed [28], making it a reliable tool to infer the dynamics governing this system.

We hypothesise that, depending on the timing and concentration at which they are added, phage and antibiotics can either act synergistically to eradicate bacteria, or to create and select for multidrug-resistant bacteria. We explore this in our model and generate guidelines to minimise the risk of generating double-antibiotic-resistant *S. aureus* when two single-resistant strains are exposed to antibiotics and phage, whilst maximising bacterial eradication.

MATERIALS AND METHODS

Laboratory methods

Bacterial strains and phage

Two *Staphylococcus aureus* strains were obtained from the Nebraska transposon library in the MRSA USA300 background [38]. These were NE327, with the *ermB* gene conferring resistance to erythromycin, and NE201KT7, a modified NE201 strain with a kanamycin resistance cassette replacing the *ermB* gene and a plasmid carrying the *tetK* gene conferring resistance to tetracycline. Horizontal gene transfer can only happen between these two strains via generalised transduction. When co-cultured with 80α phage, these give rise to double-resistant progeny (DRP) bacteria resistant to both erythromycin and tetracycline [28]. In the experiments conducted here, we used the double-resistant strain DRPET1, a DRP strain with a NE327 background generated during previous NE327, NE201KT7 and 80α co-cultures, containing both *ermB* and *tetK* genes [28]. Note that although 80α is a temperate phage, we have previously shown that lysogeny does not occur at a detectable level in our experiments, with a lysogenic frequency detection limit of 3.3×10^{-8} per non-lysogenic bacteria after 24h of co-culture, and that specialised transduction is unlikely to be responsible for horizontal gene transfer, due to the location of *tetK* on a plasmid and a ~1Mbp distance between *ermB* and the 80α integration site on the bacterial chromosome [28]. Hence the only interactions we consider between phage and bacteria in our environment are lysis and generalised transduction.

Time-kill curves

The growth conditions are identical to the ones previously used to generate data on lysis and transduction with these bacteria and phage [28]. Pre-cultures of each *S. aureus* bacterial strain (NE327, NE201KT7 and DRPET1) were separately generated overnight in 50mL conical tubes containing 10mL

135 of brain-heart infusion broth (BHIB, Sigma, UK). Unless otherwise stated, liquid cultures were
136 incubated in a warm shaking water bath (37°C, 90 rpm). Each pre-culture was then diluted in
137 phosphate-buffered saline (PBS) and mixed with 10mL of fresh BHIB in a 50mL conical tube to reach a
138 starting concentration of 10^4 colony-forming units (cfu)/mL. The new culture was incubated for 2h to
139 allow the bacteria to reach log-growth phase, following standard protocol for time-kill experiments
140 [39]. Erythromycin or tetracycline was then added to the culture, at a concentration of either 0
141 (control), 0.25, 0.5, 1, 2, 4, 8, 16, or 32 mg/L. At 0, 1, 2, 3, 4, 6 and 24h after antibiotic addition, 30µl
142 were sampled from the incubated culture, diluted in PBS, and plated on plain brain-heart infusion
143 agar. The plates were incubated overnight at 37°C. Colonies on the plates were then counted to derive
144 the concentration of bacteria in cfu/mL at the corresponding time point.

145 The experiment was repeated 3 times for each strain (NE327, NE201KT7 and DRPET1) and each
146 antibiotic (erythromycin and tetracycline).

147 Minimum inhibitory concentration

148 We measured the minimum inhibitory concentrations (MIC) of erythromycin and tetracycline for
149 NE327, NE201KT7 and DRPET1 by microbroth dilution [40]. Briefly, pre-cultures of each strain were
150 generated overnight in Mueller-Hinton broth (MHB-II, Sigma, UK). Antibiotic stocks were generated in
151 50% ethanol at concentrations doubling from 0.25 to 256 mg/L, and 10µL of each dilution were added
152 to separate wells on a 96-well plate. The overnight pre-cultures were diluted to a concentration of 10^5
153 cfu/mL, and 90µL were mixed with each antibiotic dilution in the 96-well plate. The plate was
154 incubated overnight at 37°C, and the MIC were then determined by eye, identifying the lowest
155 concentration of antibiotic which did not allow bacterial growth (i.e. the contents of the well were not
156 turbid).

157 # Modelling methods

158 All analyses were conducted in the R statistical analysis software [41]. The underlying code and data
159 are available in a GitHub repository: https://github.com/qleclerc/phage_antibiotic_dynamics.

160 ## Mathematical model description

161 We extended a previously published mathematical model of phage-bacteria dynamics, including
162 generalised transduction [28]. This original model focused on identifying the best method to capture
163 the interaction between bacteria and phage *in vitro*, in the absence of antibiotics. This model was
164 previously parameterised using the same bacterial and phage strains as in this study. Our three *S.*
165 *aureus* strains are represented: B_E (erythromycin-resistant, corresponding to *in vitro* strain NE327), B_T
166 (tetracycline-resistant, corresponding to NE201KT7), and B_{ET} (resistant to both erythromycin and
167 tetracycline, corresponding to double-resistant bacteria) (Figure 1). The model also contains 80α lytic
168 phage (P_L), which can give rise to transducing phage carrying either the erythromycin (P_E) or
169 tetracycline (P_T) resistance gene. The transducing phage only carry an antibiotic resistance gene, and
170 hence cannot lyse bacteria, but can give rise to B_{ET} bacteria via generalised transduction (Figure 1).

171 ## Antibiotic pharmacodynamics

172 We added two compartments to the model to track the concentration of antibiotics: C_E for
173 erythromycin, and C_T for tetracycline. The concentrations are expressed in mg/L. We can simulate the
174 addition of a chosen concentration of antibiotic at any given time, and the antibiotics decay at a
175 constant rate γ_E and γ_T for erythromycin and tetracycline, respectively (Figure 1). The change in
176 concentration of erythromycin over time is therefore expressed as

177 $$\frac{dC_E}{dt} = -\gamma_E \cdot C_E \, (1)$$

178 and the change in concentration of tetracycline over time is expressed as

$$\frac{dC_T}{dt} = -\gamma_T \cdot C_T \quad (2)$$

The antibiotic concentrations are then used to calculate $\varepsilon_{i,j}$, the effect of each antibiotic i (i ∈ {E, T}) on each bacterial strain j (j ∈ {E, T, ET}), according to a pharmacodynamic relationship parameterised through Hill equations [39,42], expressed as

$$\varepsilon_{i,j} = \mu_j^{max} \cdot \varepsilon_{i,j}^{max} \cdot \frac{C_i^{(H_{i,j})}}{EC50_{i,j}^{(H_{i,j})} + C_i^{(H_{i,j})}} \quad (3)$$

This commonly used function calculates the effect of an antibiotic using four parameters: the maximum effect ($\varepsilon^{max}_{i,j}$), current concentration (C_i), half maximal effective concentration ($EC50_{i,j}$), and a Hill coefficient ($H_{i,j}$). Note that $\varepsilon^{max}_{i,j}$ is relative to the maximum growth rate of the corresponding strain j (μ^{max}_j). This was necessary to ensure that these values would work with our previous estimates for bacterial growth, as these were slightly lower than the baseline growth rates estimated here (see below – "Parameter estimation").

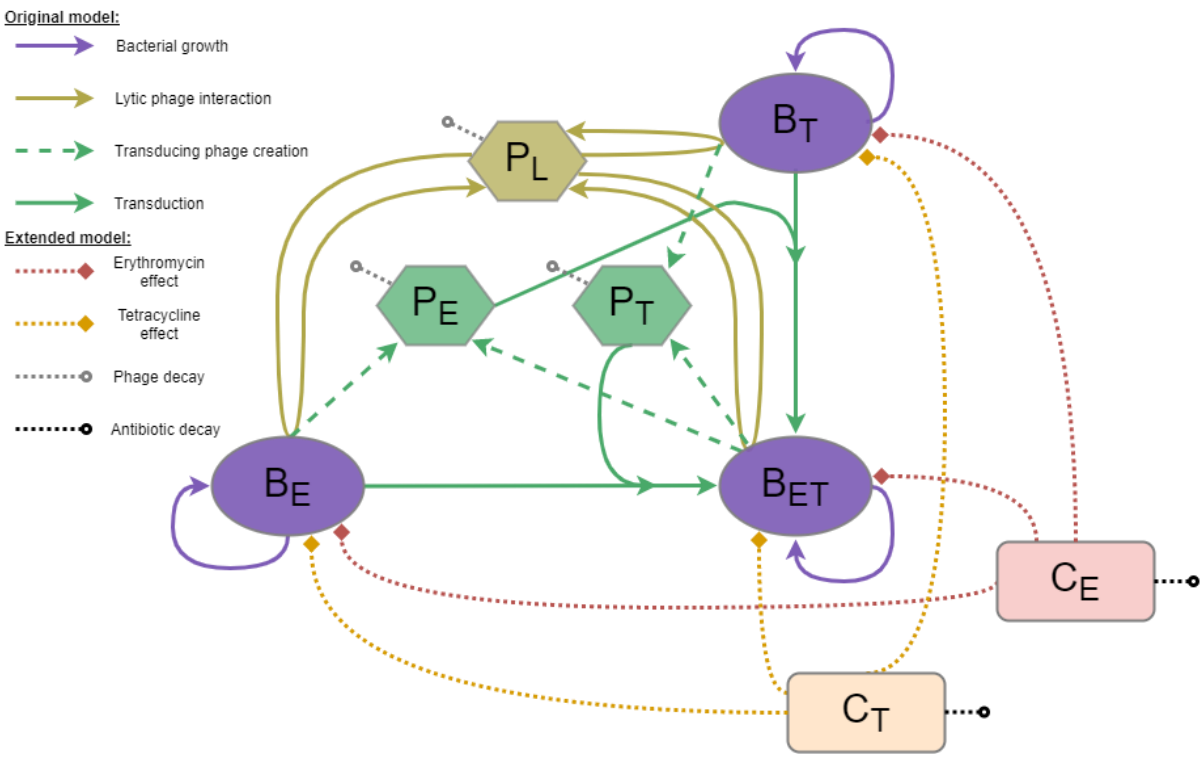

Figure 1: Mathematical model diagram. This model is an extension of our original model presented in [28], with the inclusion of antibiotic effects. Each bacteria strain (B_E resistant to erythromycin, B_T resistant to tetracycline, or B_{ET} resistant to both) can replicate (purple). The lytic phage (P_L) multiply by infecting a bacterium and bursting it to release new phage (gold). This process can create transducing phage (P_E or P_T) carrying a resistance gene (*ermB* or *tetK* respectively) taken from the infected bacterium (dashed, green). These transducing phage can then generate new double-resistant progeny (B_{ET}) by infecting the bacteria strain carrying the other resistance gene (solid, green). The antibiotics, erythromycin (C_E) and tetracycline (C_T), decrease the growth rate of each bacteria strain to varying extents, depending on their concentration and the resistance level of the strain (dotted, red and orange). Phage and antibiotics can decay at a fixed rate (dotted, grey and black).

Bacterial growth and phage predation

The bacterial growth rate μ_ϑ ($\theta \in \{E, T, ET\}$, $N = B_E+B_T+B_{ET}$) is modelled using a logistic function given by

$$\mu_\theta = \mu_\theta^{max} \cdot (1 - \frac{N}{N^{max}}) \qquad (4)$$

with a maximum growth rate of $\mu^{max}{}_\vartheta$ and carrying capacity N^{max}.

Phage predation is modelled as a frequency-dependent process. Previous work has suggested that this interaction is more biologically realistic than the more commonly used density-dependent interaction [28]. At any given time, the proportion λ of phage successfully infecting bacteria is calculated as

$$\lambda = (1 - exp\,(-\beta \cdot N)\,) \qquad (5)$$

with β representing the rate of successful phage adsorption leading to bacterial lysis, and the proportion φ_ϑ of bacteria successfully infected by the phage of type P_ϑ ($\theta \in \{L, E, T\}$) is equal to

$$\varphi_\theta = \left(1 - exp\left(-\lambda \cdot \frac{P_\theta}{N}\right)\right) \qquad (6)$$

This interaction ensures that, for any given time, the number of phage infecting bacteria and the number of bacteria infected by phage cannot be greater than the total number of phage and bacteria, respectively.

In the model, phage burst size δ_θ for each bacteria strain θ (θ ∈ {E, T, ET}) decreases from the maximum phage burst size δ^{max} as bacterial growth decreases, according to

$$\delta_\theta = \delta^{max} \cdot max\left(0, 1 - \frac{N}{N^{max}} - \frac{\varepsilon_{E,\theta}}{\mu_\theta^{max}} - \frac{\varepsilon_{T,\theta}}{\mu_\theta^{max}}\right) \qquad (7)$$

This link between phage burst size and bacterial growth was identified as the most biologically plausible explanation for the dynamics we have previously observed between the bacteria and phage in our system [28]. This decrease happens as bacteria enter stationary phase, when the population approaches carrying capacity N^{max} (as demonstrated previously [28,43,44]), but here the additional effect of antibiotics must be included. To capture this, we use the same effective scaling as the bacterial growth rate (Equation 4) with inclusion of the relative effect of antibiotics $\varepsilon_{E,\theta}$ and $\varepsilon_{T,\theta}$ in the phage burst size estimation. Since antibiotics can kill bacteria, leading to a net negative growth rate, we limit the multiplier value to 0 as a minimum, to prevent a negative burst size.

Bacteria model equations

The changes in bacteria numbers over time are given by

$$\frac{dB_E}{dt} = \mu_E \cdot \{B_E - [\omega \cdot (\varphi_L + \varphi_T) \cdot B_E]\} - (\varphi_L + \varphi_T) \cdot B_E - (\varepsilon_{E,E} + \varepsilon_{T,E}) \cdot B_E \quad (8)$$

{Change in B_E = growth of B_E – infections by P_L – infections by P_T - ery killing - tet killing}

$$\frac{dB_T}{dt} = \mu_T \cdot \{B_T - [\omega \cdot (\varphi_L + \varphi_E) \cdot B_T]\} - (\varphi_L + \varphi_E) \cdot B_T - (\varepsilon_{E,T} + \varepsilon_{T,T}) \cdot B_T \quad (9)$$

{Change in B_T = growth of B_T – infections by P_L – infections by P_E - ery killing - tet killing}

$$\frac{dB_{ET}}{dt} = \mu_{ET} \cdot [B_{ET} - (\omega \cdot \varphi_L \cdot B_{ET})] - \varphi_L \cdot B_{ET} + \varphi_E \cdot B_T + \varphi_T \cdot B_E - (\varepsilon_{E,ET} + \varepsilon_{T,ET}) \cdot B_{ET}$$

$$(10)$$

{Change in B_{ET} = growth of B_{ET} – infections by P_L + infections of B_T by P_E + infections of B_E by P_T - ery killing - tet killing}

In this model, we assume that over one time step, bacterial replication and infection by phage are mutually exclusive events, hence the repetition of the φ_ϑ terms ($\theta \in \{L, E, T\}$) on the right-hand side of Equations 8-10. As we have shown previously, this biologically plausible assumption is necessary due to the upper limits of the growth rate parameters being higher than the limits of the phage infection parameters, preventing the bacterial population from decreasing due to phage killing if this assumption is not included in the model [28]. The parameter ω represents the mutually exclusive nature of these events over one time-step in the equations, and is therefore equal to 1 (i.e. one time-step, with units of hours).

Some combinations of phage infection are not explicitly represented in the equations as they represent a flow from one compartment towards the same compartment. P_L are the lytic phage, capable of lysing all the bacteria, and are therefore included in all equations. However, the generalised transducing phage P_E and P_T only carry a bacterial antibiotic resistance gene and cannot lyse bacteria. Whilst they can infect any bacteria in our system to transfer the gene, this process will not affect bacteria already carrying the corresponding gene. For example, if a bacterium B_E is infected by a phage P_E, this bacterium remains only resistant to erythromycin, and therefore still belongs to the B_E compartment.

Phage model equations

The change in phage numbers over time are calculated as

$$\frac{dP_L}{dt} = \varphi_L(t-\tau)\cdot\delta_E\cdot(1-\alpha)\cdot\ B_E\ +$$

$$\varphi_L(t-\tau)\cdot\delta_T\cdot(1-\alpha)\cdot\ B_T\ +$$

$$\varphi_L(t-\tau)\cdot\delta_{ET}\cdot(1-2\cdot\alpha\ )\cdot\ B_{ET}\ -$$

$$\lambda\cdot P_L - \gamma_P\cdot P_L \qquad (11)$$

{Change in P_L = new P_L phage from B_E + new P_L phage from B_T + new P_L phage from B_{ET} –

P_L phage infecting bacteria – P_L decay}

$$\frac{dP_E}{dt} = \varphi_L(t-\tau)\cdot\delta_E\cdot\alpha\cdot\ B_E\ +$$

$$\varphi_L(t-\tau)\cdot\delta_{ET}\cdot\alpha\cdot\ B_{ET}\ -$$

$$\lambda\cdot P_E - \gamma_P\cdot P_E \qquad (12)$$

{Change in P_E = new P_E phage from B_E + new P_E phage from B_{ET} –

P_E phage infecting bacteria – P_E decay}

$$\frac{dP_T}{dt} = \varphi_L(t-\tau)\cdot\delta_T\cdot\alpha\cdot B_T\ +$$

$$\varphi_L(t-\tau)\cdot\delta_{ET}\cdot\alpha\cdot B_{ET}\ -$$

$$\lambda\cdot P_T - \gamma_P\cdot P_T \qquad (13)$$

{Change in P_T = new P_T phage from B_T + new P_T phage from B_{ET} –

P_T phage infecting bacteria – P_T decay}

In Equations 11-13, the latent period τ corresponds to the delay between bacterial infection and burst, and the transduction probability α corresponds to the proportion of new phage released upon burst which are transducing phage carrying the erythromycin or tetracycline resistance gene. Note that a constant rate γ_P is used for phage decay (Equations 11-13), similar to the rates used for antibiotic decay (Equations 1-2).

Parameter estimation

Parameters for bacterial growth and phage predation were originally obtained by fitting our model to *in vitro* data for the same bacteria and phage strains as in this study [28]. Briefly, the parameters were estimated using the Markov chain Monte Carlo Metropolis–Hastings algorithm. We ran the algorithm with two chains until convergence was achieved (determined using the Gelman-Rubin diagnostic, with the multivariate potential scale reduction factor < 1.2 [45]), then for each parameter we generated 50,000 samples from the posterior distributions [28].

Parameters for antibiotic effect were obtained in two steps using the least squares methods for model fitting, which aims to minimise the squared difference between data and model output. Firstly, the reduction in bacterial growth caused by a specific concentration of antibiotic ($\acute{\varepsilon}$) was obtained by fitting a deterministic growth model given by

$$\frac{d\mathrm{B}}{dt} = \mu \cdot (1 - \frac{B}{N^{max}}) \cdot \mathrm{B} - \acute{\varepsilon} \cdot B \quad (14)$$

to the bacterial concentration B over time, estimated as the mean of three *in vitro* replicates.

$\acute{\varepsilon}$ was then scaled to growth ($\varepsilon = \acute{\varepsilon}/\mu$), to represent the relative impact of the antibiotic on bacterial growth rather than an absolute value. This was necessary to ensure that these antibiotic impact values would work with our previous estimates for bacterial growth, as these were slightly lower than the

296 baseline growth rates estimated here. Since we obtained growth curve time series data for 8
297 concentrations for each strain, we generated 8 estimates of antibiotic effect for each strain.

298 Secondly, the three parameters of the Hill equation [39,42] (maximum effect ε^{max}, Hill coefficient *H*,
299 and half maximum effective concentration *EC50*), which calculates the antibiotic effect as a function
300 of concentration, were estimated by fitting Equation 3 to the 8 antibiotic effects for each strain.

301 Model scenarios considered

302 *Antibiotics alone*

303 We start with an environment containing both single-resistant strains at stationary phase (10^9 cfu/mL).
304 This mirrors the within-host diversity we could expect to see during bacterial infections [24], and the
305 fact that bacteria most often live at stationary phase in the environment [46]. We first investigate the
306 effect of the presence of either or both erythromycin and tetracycline at concentrations of 1 mg/L,
307 similar to antibiotic concentrations measured *in vivo* during treatment [47,48].

308 *Antibiotic and phage*

309 We then consider scenarios where phage are present. We first artificially inactivate transduction, by
310 setting the corresponding model parameter to 0. We add 10^9 pfu/mL of phage, similar to a
311 concentration that could be added during phage therapy, and equivalent to a multiplicity of infection
312 (ratio of phage to bacteria) of 1, similar to what could be found naturally in the environment [1]. We
313 consider scenarios where the phage are present alone, alongside only one antibiotic, or alongside both
314 antibiotics. Phage and antibiotics are assumed to be introduced concurrently at the start, and the
315 simulations run for 24h.

316 We then repeat these scenarios, but with transduction enabled to levels that were previously
317 observed *in vitro*, with approximately 1 transducing phage carrying an AMR gene generated for each
318 10^8 new lytic phage [28].

319 We repeat the analyses above with either single-resistant strain present at 10^9 cfu/mL, and the other
320 at 10^6 cfu/mL (0.1%). This could correspond to a scenario where bacterial diversity is underestimated,
321 with only one type of resistance detected [24].

322 *Antibiotic and phage level and timing variation*

323 To further investigate the scenario where transduction is enabled and both single-resistant bacterial
324 strains have a starting concentration of 10^9 cfu/mL, we vary the timing of introduction for antibiotic
325 and phage, with up to 24h delay between their respective additions, as well as varying the
326 concentration of antibiotics between 0.2 and 2.2 mg/L, and phage between 10^5 and 10^{10} pfu/mL,
327 chosen to reflect realistic ranges [1,47,48]. We run these simulations for 48h after the introduction of
328 antibiotics or phage (whichever is added first).

329 *Phage and bacteria parameters variation*

330 Finally, we vary the probability for phage to perform generalised transduction to identify threshold
331 values which dictate whether multidrug-resistant bacteria appear above detectable levels within 24h.
332 To explore the sensitivity of our results to the parameter values estimated from this single
333 environment, we also conduct a partial rank correlation to assess the effect of varying phage predation
334 parameters (adsorption rate, latent period, burst size), bacteria growth rates, and antibiotic and phage
335 decay on total bacteria remaining after 48h, and maximum double-resistant bacteria generated. This
336 allows us to generalise our conclusions as these parameters likely vary for different combinations of
337 phage, antibiotics and bacteria. The ranges evaluated are shown in Table 1, and are either derived
338 from our initial parameterisation of the model [28], or from other studies [49,50].

339 # RESULTS

340 ## *In vitro* pharmacodynamics of erythromycin and tetracycline

341 Erythromycin at all concentrations caused a decrease in erythromycin-sensitive NE201KT7 numbers
342 over 6h, but only slowed down growth for erythromycin-resistant NE327 and double-resistant
343 DRPET1, even at 32 mg/L (Figure 2). Tetracycline caused a decrease in bacterial numbers over 6h at
344 concentrations greater than 0.5 mg/L for tetracycline-sensitive NE327, 8 mg/L for tetracycline-
345 resistant NE201KT7, and 4 mg/L for DRPET1 (Figure 2). As a comparison, the minimum inhibitory
346 concentrations (MICs) of erythromycin measured by microbroth dilution were 0.25, >256 and >256
347 mg/L for NE201KT7, NE327 and DRPET1 respectively. For tetracycline, the MICs were 32, 0.25 and 32
348 mg/L for NE201KT7, NE327 and DRPET1 respectively.

349

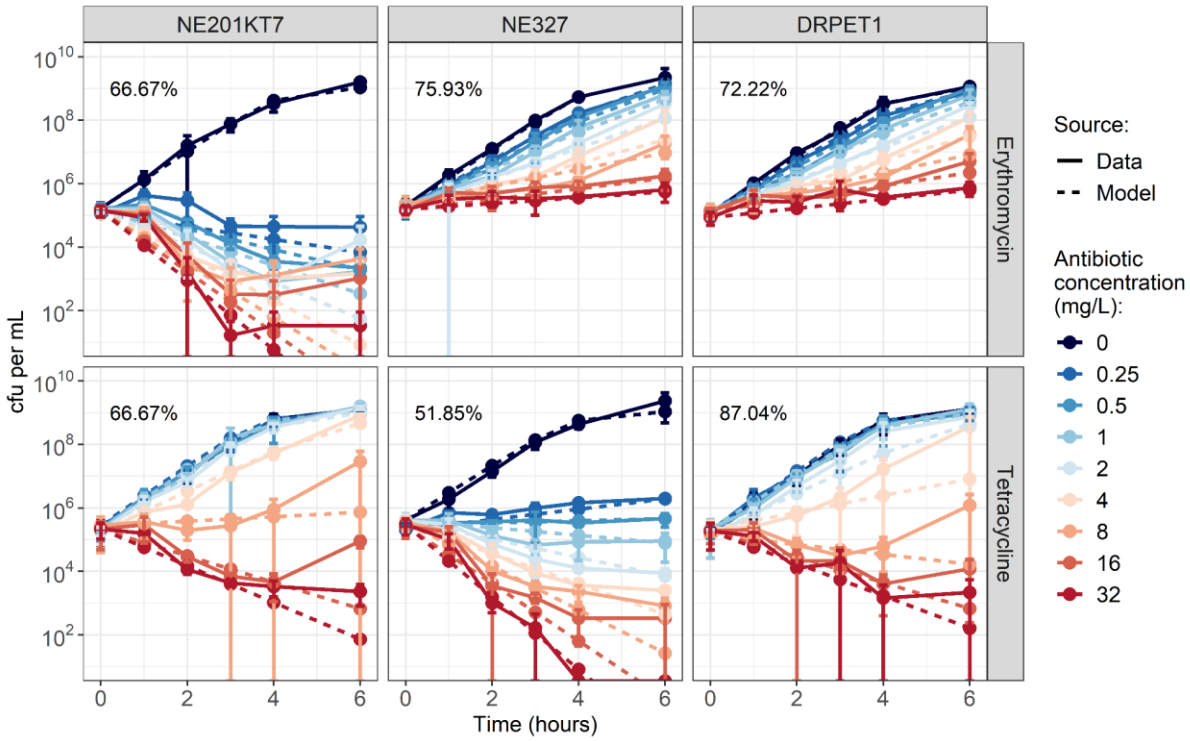

350

351 **Figure 2: Growth curves of NE201KT7 (tetracycline-resistant, left), NE327 (erythromycin-resistant,**
352 **middle) and DRPET1 (double-resistant, right), exposed to varying concentrations of erythromycin**
353 **(top) or tetracycline (bottom).** Solid lines show *in vitro* data, with error bars indicating mean +/-
354 standard deviation, from 3 replicates. Dashed lines show model output after fitting. Values indicate
355 the percentage of model points that fall within the range of the corresponding *in vitro* data point +/-
356 standard deviation. cfu: colony-forming units. Note that cfu per mL are shown on a log-scale.

357

358 The Hill equations fitted well to the effect of varying concentrations of antibiotics on the bacteria
359 (Figure 2, Figure S1). The corresponding parameter values are presented in Table 1. The antibiotic
360 effect curves for the DRPET1 are similar to the one for NE201KT7 for tetracycline and NE327 for
361 erythromycin (Figure S1), which was expected since DRPET1 contains both antibiotic-resistance genes
362 from NE201KT7 (*tetK*) and NE327 (*ermB*).

363

364

365

366

367

368

369

370

371 **Table 1: Model parameter values.** Parameters with no units are dimensionless. All estimates were

372 obtained by fitting the model to *in vitro* data, except those marked with a * which are assumed.

Name (unit)		Symbol	Estimate	Range for sensitivity analysis	Reference
Bacterial growth parameters	Carrying capacity (bacteria.mL^{-1})	N^{max}	2.76 x 10^9	-	[28]
	B_E growth rate (h^{-1})	μ^{max}_E	1.61	1.59 - 1.63	
	B_T growth rate (h^{-1})	μ^{max}_T	1.51	1.49 - 1.53	
	B_{ET} growth rate (h^{-1})	μ^{max}_{ET}	1.44	1.42 - 1.47	
Phage parameters	Phage adsorption rate (phage^{-1}.h^{-1})	β	2.3 x 10^{-10}	2.1 x 10^{-10} - 2.4 x 10^{-10}	
	Phage burst size (phage)	δ^{max}	76	70 - 83	
	Phage latent period (h)	τ	0.72	0.69 - 0.77	
	Transduction probability (phage^{-1})	α	1.0 x 10^{-8}	8.5 x 10^{-9} - 1.4 x 10^{-8}	
	Phage decay rate (h^{-1})	γ_P	0*	0 - 0.1	[49]
Antibiotic parameters	Erythromycin decay rate (h^{-1})	γ_E	0*	0 - 0.1	[50]
	Tetracycline decay rate (h^{-1})	γ_T	0*	0 - 0.1	
Effect of erythromycin on B_E	Max effect (h^{-1})	$\varepsilon^{max}_{E,E}$	1.10	-	This study
	Half maximal effective concentration (mg.L^{-1})	$EC50_{E,E}$	3.42	-	
	Hill coefficient	$H_{E,E}$	0.67	-	
Effect of erythromycin on B_T	Max effect (h^{-1})	$\varepsilon^{max}_{E,T}$	3.91	-	
	Half maximal effective concentration (mg.L^{-1})	$EC50_{E,T}$	9.26	-	
	Hill coefficient	$H_{E,T}$	0.22	-	
Effect of erythromycin	Max effect (h^{-1})	$\varepsilon^{max}_{E,ET}$	0.95	-	

on B_{ET}	Half maximal effective concentration ($mg.L^{-1}$)	$EC50_{E,ET}$	2.47	-
	Hill coefficient	$H_{E,ET}$	0.79	-
Effect of tetracycline on B_E	Max effect (h^{-1})	$\varepsilon^{max}_{T,E}$	5.40	-
	Half maximal effective concentration ($mg.L^{-1}$)	$EC50_{T,E}$	81.43	-
	Hill coefficient	$H_{T,E}$	0.30	-
Effect of tetracycline on B_T	Max effect (h^{-1})	$\varepsilon^{max}_{T,T}$	1.66	-
	Half maximal effective concentration ($mg.L^{-1}$)	$EC50_{T,T}$	7.27	-
	Hill coefficient	$H_{T,T}$	2.41	-
Effect of tetracycline on B_{ET}	Max effect (h^{-1})	$\varepsilon^{max}_{T,ET}$	1.58	-
	Half maximal effective concentration ($mg.L^{-1}$)	$EC50_{T,ET}$	4.42	-
	Hill coefficient	$H_{T,ET}$	1.70	-

Model-predicted antibacterial effect of concurrent erythromycin, tetracycline and bacteriophage presence

When simulating the dynamics of two single-resistant *S. aureus* strains in our mathematical model, as expected, the presence of only one antibiotic at 1 mg/L (4 x MIC for susceptible strains) leads to a decrease in the susceptible strain, while the resistant strain does not decrease (Figure 3a, top row). On the other hand, the presence of both antibiotics, or of only phage without transduction, causes a decrease in both bacterial strains (Figure 3a, top and middle rows). The presence of phage and one antibiotic leads to a decrease in both bacterial strains, with the antibiotic-susceptible strain decreasing faster (Figure 3a, middle row). Out of all the conditions shown here, the presence of phage and both antibiotics leads to the fastest decrease in both bacterial strains (Figure 3b). For comparison, to

384 replicate the combined effect of 10^9 pfu/mL of phage, 1 mg/L of erythromycin, and 1 mg/L of
385 tetracycline, we would need 4.58 mg/L of erythromycin and 1.14 mg/L of tetracycline in the absence
386 of phage (Figure S2).

387 Transduction does not appear to affect the antibacterial activity of antibiotics and phage when phage
388 are either present alone, alongside erythromycin, or alongside tetracycline (Figure 3a, bottom row).
389 Double-resistant progeny bacteria (B_{ET}) appear, but only reach a maximum concentration of 30
390 cfu/mL, and do not remain higher than 1 cfu/mL for more than 8h (Figure 3a, bottom row). However,
391 when both erythromycin and tetracycline are present alongside phage capable of transduction, there
392 is a steady increase in the number of B_{ET} throughout 24h, reaching 80 cfu/mL after 24h (Figure 3a,
393 bottom row & Figure 3b). It is important to note here that when both antibiotics are present, phage
394 numbers do not increase throughout the 24h period, regardless of transduction ability (Figure 3a,
395 middle and bottom rows & Figure 3b, right).

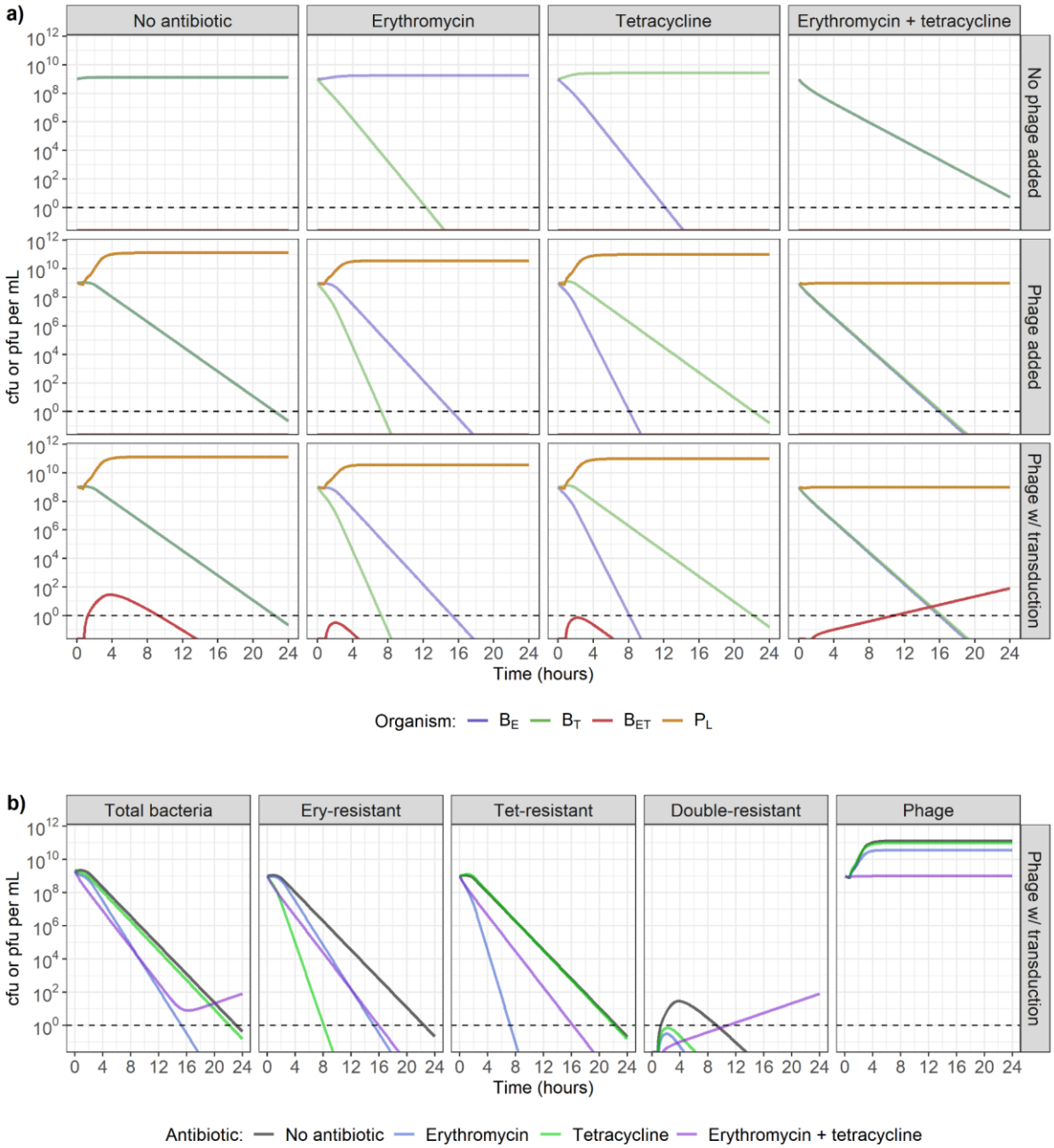

Figure 3: a) Model-predicted dynamics with two single-resistant strains starting at carrying capacity (10^9 colony-forming units (cfu)/mL), in the presence of no antibiotics (1st column), erythromycin only (2nd column), tetracycline only (3rd column), or both erythromycin and tetracycline (4th column), combined with either no phage (top row), phage incapable of transduction (middle row), or phage capable of generalised transduction (bottom row). The starting strains are either erythromycin-resistant (B_E) or tetracycline-resistant (B_T). Antibiotics and/or phage (P_L) are present at the start of the simulation, at concentrations of 1 mg/L (4 x MIC for susceptible strains) and 10^9 plaque-

404 forming units (pfu)/mL respectively. Double-resistant bacteria (B_{ET}) can be initially generated by
405 generalised transduction only, and then by replication of existing B_{ET}. Dashed line indicates the
406 detection threshold of 1 cfu or pfu/mL. **b) Change in bacteria (single-resistant to erythromycin,**
407 **single-resistant to tetracycline, or double-resistant) and phage numbers depending on the antibiotic**
408 **exposure, in the presence of phage capable of generalised transduction.** Dashed line indicates the
409 detection threshold of 1 cfu or pfu/mL.

410

411 With a reduced starting concentration of either *S. aureus* strain to 10^6 cfu/mL, while the other remains
412 at 10^9 cfu/mL, the conclusions are similar as described above, regardless of which strain is in the
413 minority. Figure 4 shows the scenario where tetracycline-resistant bacteria are in minority, and Figure
414 S3 shows the scenario where erythromycin-resistant bacteria are in minority. When erythromycin,
415 tetracycline, and phage capable of generalised transduction are all present, B_{ET} are still generated,
416 although they do not reach a concentration higher than 1 cfu/mL within 24h, instead of 11h above
417 (Figure 4, Figure 3).

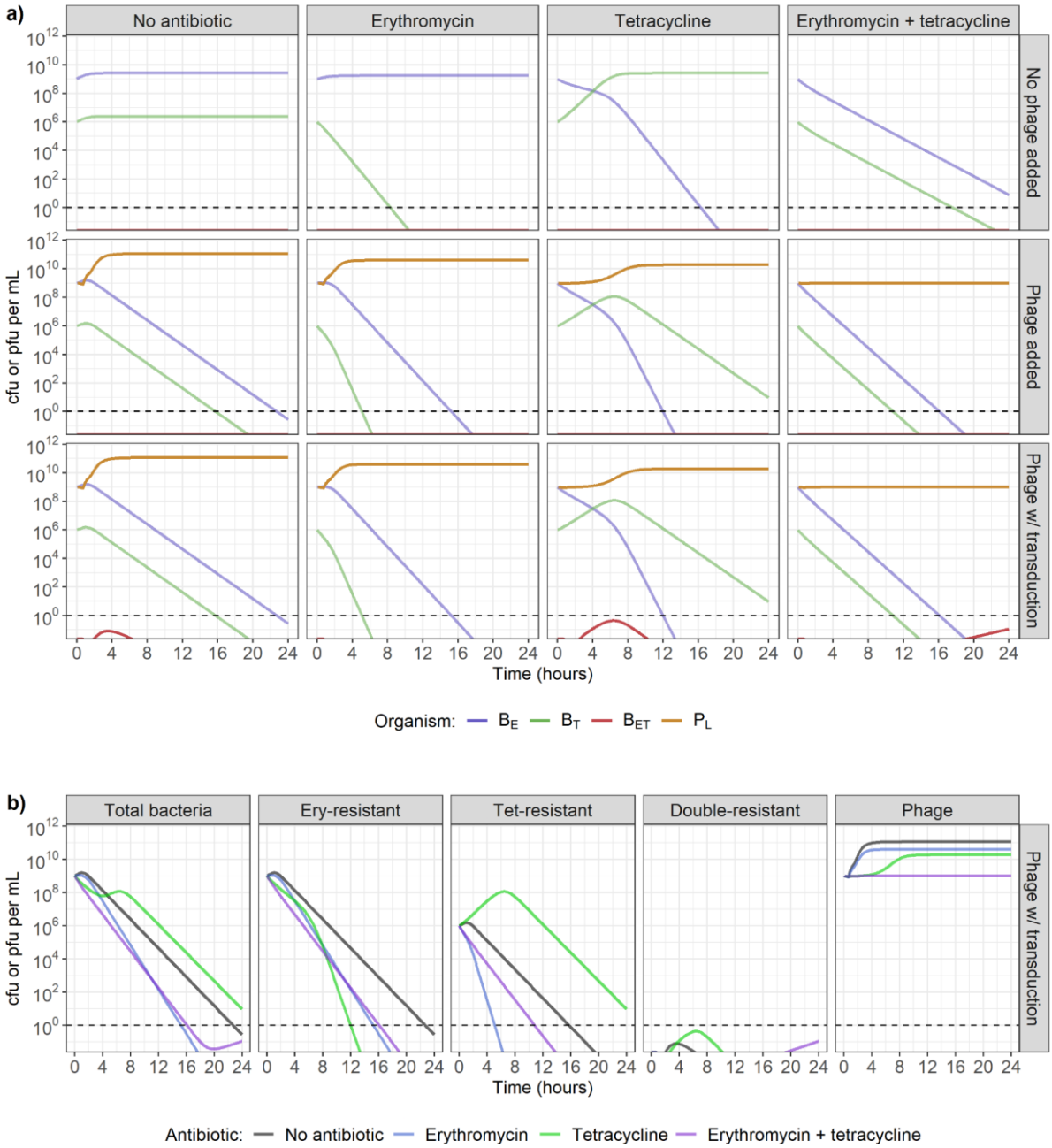

Figure 4: a) Model-predicted dynamics with one single-resistant strains starting at carrying capacity (10^9 colony-forming units (cfu)/mL) and the second in minority (10^6 cfu/mL), in the presence of no antibiotics (1st column), erythromycin only (2nd column), tetracycline only (3rd column), or both erythromycin and tetracycline (4th column), combined with either no phage (top row), phage incapable of transduction (middle row), or phage capable of generalised transduction (bottom row). Erythromycin-resistant bacteria (B_E) are initially present at a concentration of 10^9 cfu/mL, and tetracycline-resistant bacteria (B_T) at 10^6 cfu/mL. Antibiotics and/or phage (P_L) are present at the start

426 of the simulation, at concentrations of 1 mg/L (4 x MIC for susceptible strains) and 10^9 plaque-forming
427 units (pfu)/mL respectively. Double-resistant bacteria (B_{ET}) can initially be generated by generalised
428 transduction only, and then by replication of existing B_{ET}. Dashed line indicates the detection threshold
429 of 1 cfu or pfu/mL. **b) Change in bacteria (single-resistant to erythromycin, single-resistant to**
430 **tetracycline, or double-resistant) and phage numbers depending on the antibiotic exposure, in the**
431 **presence of phage capable of generalised transduction.** Dashed line indicates the detection threshold
432 of 1 cfu or pfu/mL.

433

434 Effect of variation in antibiotic and phage timing and concentration
435 on bacterial populations

436 Under conditions where both erythromycin and tetracycline are present, the timing and concentration
437 of antibiotics and phage capable of generalised transduction drives substantial variation in dynamics,
438 with failure to clear all bacteria after 48h being a possibility (Figure 5a-b, top row).

439 With a phage concentration of 10^8 cfu/mL and for any antibiotics concentration between 0.2 and 2.2
440 mg/L (Figure 5a), the optimal conditions to clear bacteria within 48h are when phage are initially
441 present, and antibiotics are introduced at least 5h later (Figure 5a, top row). However, this
442 systematically leads to B_{ET} appearance, with a peak concentration between 10 and 100 cfu/mL (Figure
443 5a, middle row), and a presence time (hours when cfu/mL > 1) of up to 10h (Figure 5a, bottom row).
444 Interestingly, if antibiotics are introduced exactly 5h after phage, the peak concentration of B_{ET} is only
445 between 1 and 10 (Figure 5a, middle row). The presence of antibiotics at the same time or shortly
446 before phage leads to failure to clear bacteria within 48h (up to between 10^8 and 10^{10} cfu/mL
447 remaining after 48h - top row), and substantial B_{ET} appearance (maximum concentration up to
448 between 10^8 and 10^{10} cfu/mL - middle row; presence time up to between 30 and 40h- bottom row).

449 Regardless of timings, the addition of at least 2.2 mg/L of antibiotics guarantees that less than 100
450 bacteria remain after 48h (top row), and no detectable B_{ET} if the antibiotics are added at least 2h
451 before the phage (bottom row).

452 When keeping the antibiotic concentrations at 1 mg/L, but varying the phage concentration, the
453 impact of the delay between phage and antibiotic presence on the bacterial population is strongly
454 dependent on phage concentration (Figure 5b). We again see that bacteria are not cleared within 48h
455 if antibiotics are present at the same time as or shortly before a concentration of phage between 10^5
456 and 10^9 pfu/mL (Figure 5b, top row). However, we now note that this also occurs if antibiotics are
457 introduced after a concentration of phage between 10^5 and 10^8 pfu/mL (Figure 5b, top row).
458 Regardless of timing, the presence of a phage concentration of more than 10^9 pfu/mL guarantees
459 bacterial clearance within 48h (top row), but leads to B_{ET} if the antibiotics are introduced after the
460 phage (maximum concentration between 10 and 100 cfu/mL - middle row; presence time between 1
461 and 10h - bottom row).

462

463

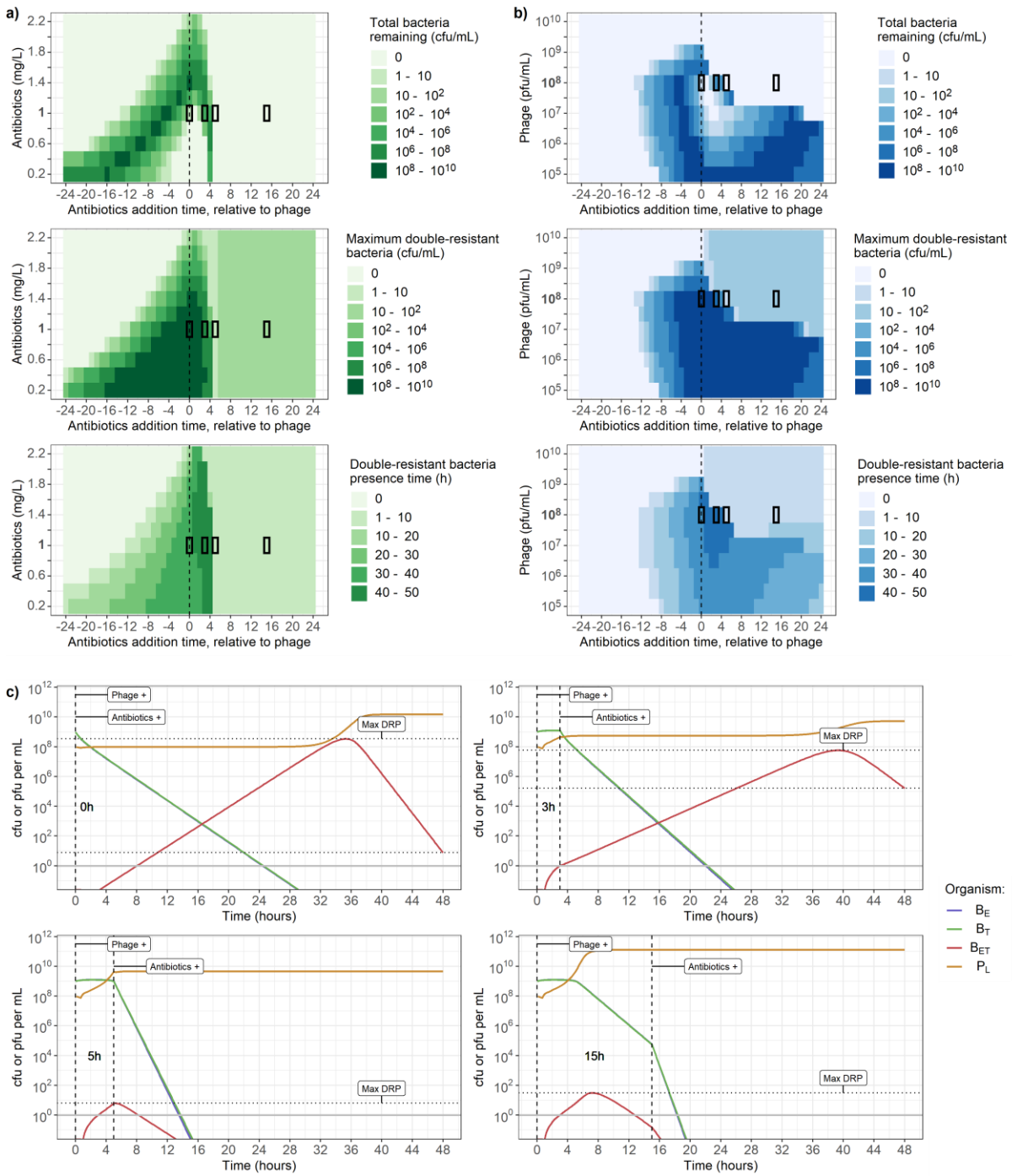

Figure 5: a-b) Varying timing (x-axis) and dose of antibiotic and phage (y-axis) affects total bacterial count after 48h (top), maximum concentration of double-resistant bacteria (B_{ET}) (middle), and time when the concentration of B_{ET} is greater than 1 colony-forming unit (cfu) per mL (bottom). a) Adding 10^8 plaque-forming units (pfu) per mL of phage, and between 0.2 and 2.2 mg/L of both erythromycin and tetracycline. **b)** Adding 1 mg/L of both erythromycin and tetracycline, and between 10^5 and 10^{10} pfu/mL of phage. The x-axis indicates the time when antibiotics were added, relative to when phage

471 were added. For example, the value "4" indicates that phage were present at the start of the
472 simulation, and antibiotics were introduced 4h later. The segments with black borders correspond to
473 the dynamics shown in c). **c) Phage and bacteria dynamics over 48h for 4 conditions taken from panel**
474 **b.** In all 4 conditions, indicated by the black rectangles, phage are initially present at a concentration
475 of 10^8 pfu/mL, while erythromycin and tetracycline are both introduced at concentrations of 1 mg/L
476 after either 0h, 3h, 5h or 15h, stated on the plots, with the timing indicated by the vertical dashed
477 lines. Horizontal dotted lines indicate bacteria remaining after 48h (corresponding to the top row of
478 a-b) and maximum double-resistant bacteria (B_{ET}) concentration (middle row of a-b). Solid line
479 indicates the detection threshold of 1 cfu or pfu/mL. The concentrations of single-resistant bacteria
480 (B_E, blue, and B_T, green) overlap and cannot be distinguished.

481

482 To investigate the dynamics behind these results, we selected four conditions from Figure 5b
483 (indicated by the 4 black rectangles) with varying antibiotic addition times and plotted the underlying
484 phage and bacteria dynamics over 48h for each (Figure 5c). In all four conditions the starting
485 concentrations are 10^8 pfu/mL for phage and 1 mg/L for antibiotics, but antibiotics are introduced
486 either 0h, 3h, 5h or 15h after phage. These plots show that if phage are increasing, they stop
487 immediately following antibiotic addition (Figure 5c, 3 and 5h delay). If antibiotics are added too soon
488 after phage (Figure 5c, 0 and 3h delay), phage do not reach a high enough number to exert a sufficient
489 killing pressure on bacteria. In that case B_{ET}, which are not substantially affected by either antibiotic,
490 replicate faster than they are killed by phage. After more than 35h, the B_{ET} population reaches a
491 sufficiently high number such that the phage population increases, and the resulting pressure is
492 enough to lead to a net negative bacterial growth rate. If antibiotics are added 15h or later after phage
493 (Figure 5b, Figure 5c), B_{ET} generation will not change, as during this period they will have already arisen
494 by transduction and been removed by phage predation. The presence of antibiotics 5h after phage is
495 optimal to ensure the lowest maximum number of B_{ET} (Figure 5c - compare horizontal dotted lines).

496 This timing allows phage to initially increase to a concentration of almost 5 x 10^9, sufficiently high to
497 exert a strong killing pressure on bacteria, while the added effect of antibiotics prevents further B_{ET}
498 generation by decreasing the single-resistant strains.

499 These results also apply to a scenario where one of the two bacterial strains is in the minority (starting
500 concentration of 10^6 instead of 10^9 cfu/mL), regardless of which strain is in the minority (Figures S4 &
501 S5). However, B_{ET} peak, presence time, and total bacteria remaining after 48h decrease faster with a
502 higher dose of antibiotic or phage, or with a higher delay between phage and antibiotics, suggesting
503 that phage and antibiotics are able to exert a greater killing pressure and generate fewer B_{ET} when one
504 strain is in the minority.

505

506 Effect of variation in phage and bacteria parameters on multidrug-
507 resistance evolution

508 Our results above rely on parameters estimated from phage and bacteria interactions *in vitro*, but
509 these may vary depending on the bacteria, phage, and environment. We can explore these different
510 conditions using our model to quantify the dynamics under varying values for parameters governing
511 phage-bacteria interactions (see Table 1 for the ranges used) to determine whether our results would
512 hold.

513 We first examine the impact of varying the transduction probability on our results (corresponding to
514 the probability that a transducing phage carrying an AMR gene is released instead of a lytic phage
515 during bacterial burst) as this is a vital and yet poorly quantified parameter. When 10^9 cfu/mL of each
516 single-resistant strain are simultaneously exposed to 10^9 pfu/mL of phage and 1 mg/L of erythromycin
517 and tetracycline, varying the transduction probability between 10^{-10} and 10^{-6} leads to a similar log-fold
518 increase in double-resistant bacteria numbers (B_{ET}, Figure 6a). Decreasing the probability only delays

519 the appearance of B_{ET} in the model, and does not prevent it. However, a probability lower than 10^{-9}
520 may prevent the appearance of B_{ET} in reality, since the single-resistant strains become undetectable
521 (< 1 cfu/mL) before the B_{ET} become detectable. If antibiotics are added more than 10h after phage, B_{ET}
522 will have already started declining due to phage predation, hence the antibiotics only contribute to
523 further increasing the decline in bacterial numbers (Figure 5, Figure 6b). Under these conditions, a
524 transduction probability lower than 10^{-9} is necessary to prevent B_{ET} from increasing past the detection
525 threshold (1 cfu/mL) (Figure 6b). If antibiotics are introduced 10h before phage, the resulting decline
526 in single-resistant bacteria prevents any B_{ET} from reaching a detectable level before single-resistant
527 bacteria are eradicated (< 1 cfu/mL), even with the highest transduction probability of 10^{-6} (Figure 6c).

528 Looking at how changes in other phage and bacteria parameters may affect our results, partial rank
529 correlation shows that an increase in phage predation either through an increase in phage adsorption
530 rate (β) or phage burst size (δ^{max}) correlates with a decrease in maximum B_{ET} detected over 48h (Figure
531 6d, blue). For example, the correlation coefficient of -0.65 between β and maximum B_{ET} implies that a
532 100% increase in adsorption rate is correlated with a 65% decrease in maximum double-resistant
533 bacteria detected over 48h. An increase in phage burst size is also correlated with a decrease in
534 bacteria remaining after 48h. However, adsorption rate is not substantially correlated with bacteria
535 remaining after 48h (Figure 6d, red). Finally, an increase in latent period (τ), equivalent to a decrease
536 in predation since phage will take longer before lysing the bacteria, is correlated with an increase in
537 maximum B_{ET}, but is not substantially correlated with bacteria remaining after 48h.

538 Although we were not able to parameterise our model for antibiotic decay, our 24h time-kill curves
539 suggest that antibiotics no longer decrease bacterial numbers after 24h (Figure S6). Phage may also
540 be affected by decay in the environment. Hence, we included these parameters in our partial rank
541 correlation analysis. An increase in phage or antibiotic decay (γ_P, γ_E, γ_T) is correlated with an increase
542 in maximum B_{ET} (Figure 6d, blue), but unexpectedly with a decrease in bacteria remaining after 48h
543 (Figure 6d, red). This is explained by the fact that such an increase leads to a weakened killing pressure

544 on B_{ET}, which are able to increase faster. This translates to a shorter time before the phage population
545 is able to increase again due to enough bacteria being available for predation, and thus a shorter time
546 before B_{ET} start decreasing due to phage killing (Figure S7). This also explains why an increase in the
547 transduction probability (α) is correlated with a decrease in bacteria remaining after 48h, as it leads
548 to a faster increase in B_{ET}, and thus a shorter time before the phage are able to increase and eradicate
549 the B_{ET} population. Finally, single-resistant bacterial growth rates (μ^{max}_{E}, μ^{max}_{T}) are not substantially
550 correlated with either maximum B_{ET} or remaining bacteria, while double-resistant growth rate (μ^{max}_{ET})
551 is only weakly positively correlated with maximum B_{ET}, and negatively with remaining bacteria.

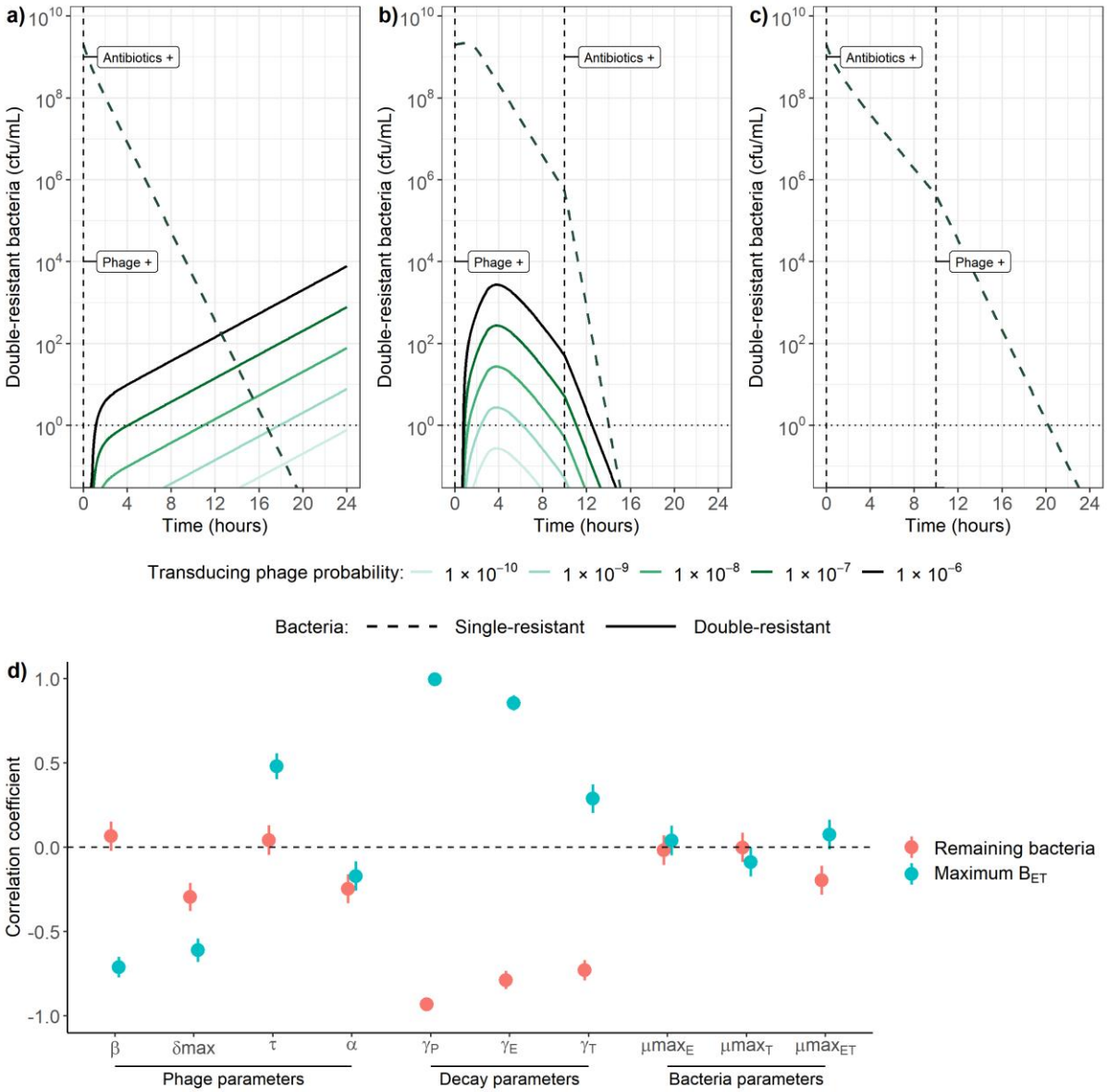

552

553 **Figure 6: Sensitivity of phage-bacteria dynamics to changes in model parameters. Effect of varying**
554 **the transduction probability between 10^{-10} and 10^{-6} when a) antibiotics and phage are present at the**
555 **start of the simulation, b) phage are present at the start, antibiotics are introduced 10h later, and c)**
556 **antibiotics are present at the start, phage are added 10h later.** Transduction probability is defined as
557 the probability that a transducing phage carrying an AMR gene is released instead of a lytic phage
558 during bacterial burst. The dashed lines for single-resistant bacteria overlap and cannot be
559 distinguished. Vertical dashed lines indicate timing of addition of antibiotics or phage. cfu/mL: colony-
560 forming units per mL. **d) Partial rank correlation between model parameters, and remaining bacteria**
561 **after 48h (pink) or maximum double-resistant bacteria (B_{ET}) concentration (blue).** Information on the
562 parameter ranges investigated can be found in Table 1. β: adsorption rate, δ^{max}: burst size, τ: latent
563 period, α: transduction probability, γ_P: phage decay, γ_E: erythromycin decay, γ_T: tetracycline decay,
564 μ^{max}_E: B_E growth rate, μ^{max}_T: B_T growth rate, μ^{max}_{ET}: B_{ET} growth rate.

DISCUSSION

Summary of results

In this work, we reconcile the existing literature suggesting either that phage and antibiotics can synergistically kill bacteria, or that antibiotics reduce the efficacy of phage predation, whilst also considering the synergy of phage and antibiotics on antimicrobial resistance (AMR) evolution. We showed that although phage replication is limited in the presence of antibiotics, which negatively affect bacterial growth, phage are still able to exert a strong killing pressure on bacteria to complement the action of antibiotics. Under such conditions, the concentration and timing of antibiotics and phage are essential: phage introduced after antibiotics at a low concentration may not be able to replicate and hence not contribute to killing the bacterial population. Phage and antibiotics can act synergistically to drive AMR evolution when phage generate multidrug-resistant bacteria by transduction, and antibiotics act as a selection pressure. This is again exacerbated by the reduction in phage replication caused by antibiotics: a low concentration of phage capable of transduction introduced after antibiotics will not exert a strong killing pressure on bacteria, and instead generate multidrug-resistant bacteria at a background rate which are then selected for by the antibiotics.

Optimal conditions to clear bacteria and minimise AMR evolution

The best conditions to guarantee bacterial eradication within 48h whilst minimising the risk of multidrug-resistant bacteria evolution in our system are when antibiotics are present before phage, and either when erythromycin and tetracycline are present at a concentration of at least 2 mg/L (8 x MIC for susceptible strains), or phage at a concentration of at least 10^{10} pfu/mL (Figure 5a-b). Multidrug-resistant bacteria generation is also restricted if phage are introduced at least 10h after antibiotics (Figure 5a-b). This may be particularly relevant in the context of antibacterial treatment,

587 further discussed below. The worst outcome in which antibiotics and phage fail to rapidly clear all
588 bacteria and instead act synergistically to drive AMR evolution is a combination of a low antibiotic
589 dose (< 1 mg/L) with a low phage dose (< 10^9 pfu/ml), introduced around the same time (Figure 5a-b).
590 Unfortunately, this may correspond to values seen in natural environments where phage are
591 commonly found and antibiotics are residually present due to pollution [2,3].

592 Importance of transduction in the environment and during phage 593 therapy

594 Our results highlight the necessity to better understand the role of transduction in AMR spread and
595 evolution, and not assume by default that it is too rare to be relevant compared to other mechanisms
596 of horizontal gene transfer such as conjugation and transformation. We found that multidrug-
597 resistance evolution remained possible even at the lowest probability we considered here of a
598 transducing phage carrying an AMR gene being released instead of a lytic phage during burst (1
599 transducing phage per 10^9 lytic phage). Additionally, in this work we assumed that transduction rates
600 are constant, but previous research has shown that sub-MIC antibiotic exposure can lead to an
601 increase in transducing phage, but not lytic ones [51]. Hence, our results may still underestimate the
602 relative impact of transduction versus predation by phage when antibiotics are present. However, our
603 findings are encouraging for conditions under which AMR evolution is limited, since even with a high
604 risk of transduction (1 transducing phage per 10^6 lytic phage), if phage are only introduced to an
605 environment more than 10h after antibiotics, multidrug-resistant bacteria do not reach detectable
606 levels before single-resistant strains are eradicated (Figure 6c).

607 To the best of our knowledge, our model is the first to consider the potential consequences of
608 transduction in a system where concentrations of bacteria, phage, and antibiotic are similar to those
609 we may see during phage therapy. Previously our work only considered bacteria and phage capable
610 of generalised transduction in the absence of antibiotics [28], whilst others have explored bacteria

611 phage and antibiotics without including generalised transduction [6–8,10]. We echo the conclusions
612 from these previous studies which highlighted that the timing of antibiotics and phage introduction
613 during phage therapy can affect the rate at which bacteria are cleared, but extend these to show that
614 timing may also impact the risk for multidrug-resistant bacteria to be generated. Here, we suggest
615 that, although both sequential treatments can ultimately lead to bacterial eradication, the timing leads
616 to a trade-off between a slower clearing rate of bacteria (if antibiotics are added before phage), and
617 a higher risk of multidrug-resistance evolution (if phage are added before antibiotics). Future studies
618 and clinical trials of phage therapy should investigate varying timings of phage and antibiotics, instead
619 of only investigating their simultaneous application, and consider the risk of transduction during
620 treatment.

621 In any case, our ability to measure the impact of transduction as a driver of AMR evolution *in vivo* is
622 currently limited since individuals are not routinely screened for phage. A first step to measure this
623 despite the limitation may be to investigate evidence for within-patient changes in the resistance
624 profile of *S. aureus* isolates, as these would likely be caused by transduction [23]. In the case of
625 antibiotic treatment, the natural presence of phage capable of transduction may explain instances of
626 treatment failure, if these generate multidrug-resistant strains which are then selected for by the
627 antibiotics. Future studies monitoring therapeutic outcomes of antibacterial treatment in patients
628 where phage are also detected will be essential to better understand how our findings translate to *in*
629 *vivo* settings.

630 Limitations

631 The major limitation of our work is the deterministic nature of our model. While it does not account
632 for stochastic events which would play a large role when bacterial numbers are low, the deterministic
633 model is useful for analysis purposes, as it represents the average scenario we would observe. In
634 reality, we would likely see either bacterial clearance or unexpected increases at low numbers of

635 bacteria. We only generated model predictions for up to 48h, as our parameter values were obtained
636 using data from experiments over 24h. Beyond this time, bacteria and phage may be affected
637 negatively due to resource depletion, depending on the environment.

638 Our model does not include some dynamics which may be present *in vivo*, as we do not currently have
639 robust data available to parameterise these features, and would instead have had to rely on
640 assumptions or previously estimated parameter values from different settings. Notably, we have not
641 included the effect of the immune system, which may limit the number of multidrug-resistant bacteria
642 generated as it could suppress both bacteria and phage populations *in vivo* [52,53]. If the model was
643 extended to include the immune system, it would also have to consider potential detrimental effects
644 of large doses of phage and antibiotics, which would restrict these concentrations to prevent side
645 effects *in vivo* [54,55].

646 In addition, we assume that all the bacteria in our environment are equally susceptible to phage
647 infection, and have not considered the possibility for any further evolution. This includes adaptation
648 mutation allowing multidrug-resistant bacteria to overcome any fitness cost, as well as resistance to
649 phage. In our own previous *in vitro* experiments using these *S. aureus* strains and phage, we did not
650 detect evidence of bacterial resistance to phage appearing within 24h [28]. However, such resistance
651 may arise over longer periods of time [56,57]. The threat represent by phage resistance evolution is
652 clear for multidrug-resistant bacteria, as these would then no longer be affected by either antibiotics
653 nor phage. On the other hand, if single antibiotic-resistant strains developed resistance to phage in
654 our system, they would still be removed by the other antibiotic they are susceptible to, but may then
655 be more likely to benefit from transduction and become multidrug-resistant, depending on the phage
656 resistance mechanism. If resistance occurs by targeting and neutralising phage DNA in the cell (e.g.
657 CRISPR-Cas [57]), bacterial DNA injected by a transducing phage would not be targeted, hence
658 protecting the resistant bacteria from phage lytic infection whilst still allowing transduction. However,
659 if resistance occurs by preventing of phage binding (e.g. surface receptor modification [57], although

660 there is limited evidence of this type of phage resistance in *S. aureus* [58]), then the bacteria would no
661 longer benefit from transduction. In any case, the risk of phage resistance could be mitigated by rapid
662 killing of bacteria, before phage resistance arises, highlighting the importance of measuring how fast
663 bacterial eradication occurs.

664 Although we varied the concentration of antibiotics in our results, we have consistently added
665 erythromycin and tetracycline in equal amounts. Our model would allow us to change this, yet we
666 have chosen not to for simplicity and because the antibacterial effect curves look similar for these two
667 antibiotics in our setting (Figure S1). However, for other antibiotics it may be necessary to revisit this
668 assumption and investigate concentrations which may better reflect those to which bacteria are
669 exposed to in the environment or during antibacterial treatment.

670 Generalisability

671 Our model is extensively parameterised using data from a single phage and three *S. aureus* strains,
672 making it a robust tool to study the dynamics of these organisms, as it relies on a minimum number
673 of assumptions [28]. However, the parameters we have estimated (adsorption rate, burst size, latent
674 period and transduction probability) will likely vary depending on the phage, bacteria, and
675 environment studied. Our sensitivity analysis shows that the model outputs are reasonable with
676 alternative parameter values, predicting for example that phage with a higher predation capacity
677 (higher adsorption rate or burst size, or lower latent period) would clear more bacteria within 48h,
678 and reduce the maximum number of multidrug-resistant bacteria generated. This model has been
679 developed as part of an interdisciplinary project alongside *in vitro* experiments, hence it could be easily
680 re-parameterised using data for other strains of bacteria and phage showing similar dynamics of lysis
681 and generalised transduction. The structure of the model is generalisable to other systems of
682 generalised transducing phage and bacteria, as it captures the relevant biological characteristics of
683 phage predation and generalised transduction [28].

684 ## The unique dynamics of phage, bacteria, and antibiotics

685 We suggest that transduction and the effect of antibiotics should be considered in the context of the
686 previously described unique dynamics of phage and bacteria. These imply that phage must first reach
687 a certain concentration (previously referred to as "inundation threshold") before they can offset
688 bacterial growth and decrease the bacterial population, and bacteria must first reach a certain
689 concentration ("proliferation threshold") before the phage population can increase [10]. Generalised
690 transduction and antibiotics affect the size of the bacterial population, and therefore how phage
691 interact with bacteria to clear them and generate multidrug-resistant bacteria. Thus, multidrug-
692 resistant bacteria are able to increase in our model if phage are initially present at a concentration
693 lower than the inundation threshold (Figure 5c). This also explains our counterintuitive observation
694 that higher decay rates may lead to less bacteria remaining after 48h (Figure 6d), as this would allow
695 bacteria to reach the proliferation threshold sooner, and therefore allow phage to increase up to the
696 inundation threshold sooner (Figure S7). Importantly, our results similarly suggest that higher decay
697 rates for antibiotics present alongside phage would reduce bacteria remaining after 48h, at the cost
698 of a higher peak concentration of multidrug-resistant bacteria, since this decay would allow bacteria
699 to reach the proliferation threshold sooner (Figure 6c, Figure S7). This knowledge may be further
700 useful in the context of phage therapy, to select the antibiotics that will be given alongside phage [50].

701 ## Conclusions

702 Our results demonstrate the complex synergy between phage and antibiotics to kill bacteria and drive
703 the evolution of AMR. We suggest this synergy leads to a trade-off between a slower clearing rate of
704 bacteria (if antibiotics are added before phage), and a higher risk of multidrug-resistance evolution (if
705 phage are added before antibiotics), further exacerbated by low concentrations of either phage or
706 antibiotics. Interdisciplinary frameworks such as ours combining *in vitro* data and mathematical
707 models are key to understanding both fundamental AMR evolution, and new interventions like phage

708 therapy or screening for phage in patients. Our conclusions form hypotheses to guide future
709 experimental and clinical work, notably for studies of phage therapy which should consider the risk
710 for multidrug-resistance evolution by transduction, and investigate varying timings and
711 concentrations of phage and antibiotics instead of only their simultaneous use.

ACKNOWLEDGMENTS

The authors would like to thank Caroline Memmi for helpful discussions on antibiotic bioavailability and *in vivo* antibiotic concentrations, as well as Joseph Standing and his research group for advice regarding antibiotic pharmacodynamics modelling.

FUNDING

Q.J.L was supported by a studentship from the Medical Research Council Intercollegiate Doctoral Training Program (MR/N013638/1). G.M.K was supported by a Skills Development Fellowship from the Medical Research Council (MR/P014658/1). G.M.K and J.A.L were supported by a Research Grant from the Medical Research Council (MR/P028322/1). The funders played no role in the study design, data collection and analysis, decision to publish, or preparation of the manuscript.

REFERENCES

1. Clokie MRJ, Millard AD, Letarov AV, Heaphy S. Phages in nature. Bacteriophage. 2011;1: 31–45. doi:10.4161/bact.1.1.14942

2. Batinovic S, Wassef F, Knowler SA, Rice DTF, Stanton CR, Rose J, et al. Bacteriophages in Natural and Artificial Environments. Pathogens. 2019;8: 100. doi:10.3390/pathogens8030100

3. Larsson DGJ. Pollution from drug manufacturing: review and perspectives. Philos Trans R Soc B Biol Sci. 2014;369: 20130571. doi:10.1098/rstb.2013.0571

4. Brives C, Pourraz J. Phage therapy as a potential solution in the fight against AMR: obstacles and possible futures. Palgrave Commun. 2020;6: 1–11. doi:10.1057/s41599-020-0478-4

5. Li X, He Y, Wang Z, Wei J, Hu T, Si J, et al. A combination therapy of Phages and Antibiotics: Two is better than one. Int J Biol Sci. 2021;17: 3573–3582. doi:10.7150/ijbs.60551

6. Berryhill BA, Huseby DL, McCall IC, Hughes D, Levin BR. Evaluating the potential efficacy and limitations of a phage for joint antibiotic and phage therapy of Staphylococcus aureus infections. Proc Natl Acad Sci. 2021;118. doi:10.1073/pnas.2008007118

7. Lopes A, Pereira C, Almeida A. Sequential Combined Effect of Phages and Antibiotics on the Inactivation of Escherichia coli. Microorganisms. 2018;6: 125. doi:10.3390/microorganisms6040125

8. Torres-Barceló C, Arias-Sánchez FI, Vasse M, Ramsayer J, Kaltz O, Hochberg ME. A Window of Opportunity to Control the Bacterial Pathogen Pseudomonas aeruginosa Combining Antibiotics and Phages. PLoS ONE. 2014;9: e106628. doi:10.1371/journal.pone.0106628

9. Abedon ST. Phage-Antibiotic Combination Treatments: Antagonistic Impacts of Antibiotics on the Pharmacodynamics of Phage Therapy? Antibiotics. 2019;8: 182. doi:10.3390/antibiotics8040182

10. Payne RJH, Jansen VAA. Understanding Bacteriophage Therapy as a Density-dependent Kinetic Process. J Theor Biol. 2001;208: 37–48. doi:10.1006/jtbi.2000.2198

11. Wang L, Tkhilaishvili T, Bernal Andres B, Trampuz A, Gonzalez Moreno M. Bacteriophage–antibiotic combinations against ciprofloxacin/ceftriaxone-resistant Escherichia coli in vitro and in an experimental Galleria mellonella model. Int J Antimicrob Agents. 2020;56: 106200. doi:10.1016/j.ijantimicag.2020.106200

12. Kumaran D, Taha M, Yi Q, Ramirez-Arcos S, Diallo J-S, Carli A, et al. Does Treatment Order Matter? Investigating the Ability of Bacteriophage to Augment Antibiotic Activity against Staphylococcus aureus Biofilms. Front Microbiol. 2018;9: 127. doi:10.3389/fmicb.2018.00127

13. Chaudhry WN, Concepción-Acevedo J, Park T, Andleeb S, Bull JJ, Levin BR. Synergy and Order Effects of Antibiotics and Phages in Killing Pseudomonas aeruginosa Biofilms. PLoS ONE. 2017;12: e0168615. doi:10.1371/journal.pone.0168615

14. von Wintersdorff CJH, Penders J, van Niekerk JM, Mills ND, Majumder S, van Alphen LB, et al. Dissemination of Antimicrobial Resistance in Microbial Ecosystems through Horizontal Gene Transfer. Front Microbiol. 2016;7. doi:10.3389/fmicb.2016.00173

15. Fernández L, Rodríguez A, García P. Phage or foe: an insight into the impact of viral predation on microbial communities. ISME J. 2018;12: 1171–1179. doi:10.1038/s41396-018-0049-5

16. Balcázar JL. How do bacteriophages promote antibiotic resistance in the environment? Clin Microbiol Infect. 2018;24: 447–449. doi:10.1016/j.cmi.2017.10.010

17. Haaber J, Penadés JR, Ingmer H. Transfer of Antibiotic Resistance in Staphylococcus aureus. Trends Microbiol. 2017;25: 893–905. doi:10.1016/j.tim.2017.05.011

18. Leclerc QJ, Lindsay JA, Knight GM. Mathematical modelling to study the horizontal transfer of antimicrobial resistance genes in bacteria: current state of the field and recommendations. J R Soc Interface. 2019;16: 20190260. doi:10.1098/rsif.2019.0260

19. Verheust C, Pauwels K, Mahillon J, Helinski DR, Herman P. Contained use of Bacteriophages: Risk Assessment and Biosafety Recommendations. Appl Biosaf. 2010;15: 32–44. doi:10.1177/153567601001500106

20. Jassim SAA, Limoges RG. Natural solution to antibiotic resistance: bacteriophages 'The Living Drugs.' World J Microbiol Biotechnol. 2014;30: 2153–2170. doi:10.1007/s11274-014-1655-7

774 21. Chen J, Quiles-Puchalt N, Chiang YN, Bacigalupe R, Fillol-Salom A, Chee MSJ, et al. Genome
775 hypermobility by lateral transduction. Science. 2018;362: 207–212.
776 doi:10.1126/science.aat5867

777 22. den Heijer CDJ, van Bijnen EME, Paget WJ, Pringle M, Goossens H, Bruggeman CA, et al.
778 Prevalence and resistance of commensal Staphylococcus aureus, including meticillin-resistant S
779 aureus, in nine European countries: a cross-sectional study. Lancet Infect Dis. 2013;13: 409–415.
780 doi:10.1016/S1473-3099(13)70036-7

781 23. Lindsay JA. Staphylococcus aureus genomics and the impact of horizontal gene transfer. Int J
782 Med Microbiol. 2014;304: 103–109. doi:10.1016/j.ijmm.2013.11.010

783 24. Stanczak-Mrozek KI, Manne A, Knight GM, Gould K, Witney AA, Lindsay JA. Within-host diversity
784 of MRSA antimicrobial resistances. J Antimicrob Chemother. 2015;70: 2191–2198.
785 doi:10.1093/jac/dkv119

786 25. Tacconelli E, Carrara E, Savoldi A, Harbarth S, Mendelson M, Monnet DL, et al. Discovery,
787 research, and development of new antibiotics: the WHO priority list of antibiotic-resistant
788 bacteria and tuberculosis. Lancet Infect Dis. 2018;18: 318–327. doi:10.1016/S1473-
789 3099(17)30753-3

790 26. Rice LB. Federal Funding for the Study of Antimicrobial Resistance in Nosocomial Pathogens: No
791 ESKAPE. J Infect Dis. 2008;197: 1079–1081. doi:10.1086/533452

792 27. Cassini A, Högberg LD, Plachouras D, Quattrocchi A, Hoxha A, Simonsen GS, et al. Attributable
793 deaths and disability-adjusted life-years caused by infections with antibiotic-resistant bacteria in
794 the EU and the European Economic Area in 2015: a population-level modelling analysis. Lancet
795 Infect Dis. 2019;19: 56–66. doi:10.1016/S1473-3099(18)30605-4

796 28. Leclerc QJ, Wildfire J, Gupta A, Lindsay JA, Knight GM. Growth-Dependent Predation and
797 Generalized Transduction of Antimicrobial Resistance by Bacteriophage. mSystems. 2022;0:
798 e00135-22. doi:10.1128/msystems.00135-22

799 29. McCarthy AJ, Loeffler A, Witney AA, Gould KA, Lloyd DH, Lindsay JA. Extensive Horizontal Gene
800 Transfer during Staphylococcus aureus Co-colonization In Vivo. Genome Biol Evol. 2014;6: 2697–
801 2708. doi:10.1093/gbe/evu214

802 30. Fish R, Kutter E, Wheat G, Blasdel B, Kutateladze M, Kuhl S. Bacteriophage treatment of
803 intransigent diabetic toe ulcers: a case series. J Wound Care. 2016;25: S27–S33.
804 doi:10.12968/jowc.2016.25.Sup7.S27

805 31. Lehman SM, Mearns G, Rankin D, Cole RA, Smrekar F, Branston SD, et al. Design and Preclinical
806 Development of a Phage Product for the Treatment of Antibiotic-Resistant Staphylococcus
807 aureus Infections. Viruses. 2019;11: 88. doi:10.3390/v11010088

808 32. Ngassam-Tchamba C, Duprez JN, Fergestad M, De Visscher A, L'Abee-Lund T, De Vliegher S, et
809 al. In vitro and in vivo assessment of phage therapy against Staphylococcus aureus causing
810 bovine mastitis. J Glob Antimicrob Resist. 2020;22: 762–770. doi:10.1016/j.jgar.2020.06.020

811 33. Ooi ML, Drilling AJ, Morales S, Fong S, Moraitis S, Macias-Valle L, et al. Safety and Tolerability of
812 Bacteriophage Therapy for Chronic Rhinosinusitis Due to Staphylococcus aureus. JAMA
813 Otolaryngol Neck Surg. 2019;145: 723–729. doi:10.1001/jamaoto.2019.1191

814 34. Petrovic Fabijan A, Lin RCY, Ho J, Maddocks S, Ben Zakour NL, Iredell JR. Safety of bacteriophage
815 therapy in severe Staphylococcus aureus infection. Nat Microbiol. 2020;5: 465–472.
816 doi:10.1038/s41564-019-0634-z

817 35. Raj JRM, Karunasagar I. Phages amid antimicrobial resistance. Crit Rev Microbiol. 2019;45: 701–
818 711. doi:10.1080/1040841X.2019.1691973

819 36. Hassan AY, Lin JT, Ricker N, Anany H. The Age of Phage: Friend or Foe in the New Dawn of
820 Therapeutic and Biocontrol Applications? Pharmaceuticals. 2021;14: 199.
821 doi:10.3390/ph14030199

822 37. Rodríguez-Rubio L, Jofre J, Muniesa M. Is Genetic Mobilization Considered When Using
823 Bacteriophages in Antimicrobial Therapy? Antibiotics. 2017;6: 32.
824 doi:10.3390/antibiotics6040032

825 38. Fey PD, Endres JL, Yajjala VK, Widhelm TJ, Boissy RJ, Bose JL, et al. A Genetic Resource for Rapid
826 and Comprehensive Phenotype Screening of Nonessential Staphylococcus aureus Genes. mBio.
827 2013;4. doi:10.1128/mBio.00537-12

828 39. Mouton JW, Vinks AA. Pharmacokinetic/Pharmacodynamic Modelling of Antibacterials In Vitro
829 and In Vivo Using Bacterial Growth and Kill Kinetics. Clin Pharmacokinet. 2005;44: 201–210.
830 doi:10.2165/00003088-200544020-00005

831 40. Wayne P, Clinical and Laboratory Standards Institute. CSLI document M07-A9. 9th ed. Methods
832 for Dilution Antimicrobial Susceptibility Tests for Bacteria That Grow Aerobically; Approved
833 Standard. 9th ed. CSLI; 2012.

834 41. R Core Team. R: A Language and Environment for Statistical Computing. Vienna, Austria: R
835 Foundation for Statistical Computing; 2020. Available: https://www.R-project.org/

836 42. Regoes RR, Wiuff C, Zappala RM, Garner KN, Baquero F, Levin BR. Pharmacodynamic Functions:
837 a Multiparameter Approach to the Design of Antibiotic Treatment Regimens. Antimicrob Agents
838 Chemother. 2004;48: 3670–3676. doi:10.1128/AAC.48.10.3670-3676.2004

839 43. Weld RJ, Butts C, Heinemann JA. Models of phage growth and their applicability to phage
840 therapy. J Theor Biol. 2004;227: 1–11.

841 44. Schrag SJ, Mittler JE. Host-Parasite Coexistence: The Role of Spatial Refuges in Stabilizing
842 Bacteria-Phage Interactions. Am Nat. 1996;148: 348–377. doi:10.1086/285929

843 45. Gelman A, Rubin DB. Inference from Iterative Simulation Using Multiple Sequences. Stat Sci.
844 1992;7: 457–472.

845 46. Gefen O, Fridman O, Ronin I, Balaban NQ. Direct observation of single stationary-phase bacteria
846 reveals a surprisingly long period of constant protein production activity. Proc Natl Acad Sci.
847 2014;111: 556–561. doi:10.1073/pnas.1314114111

848 47. Krasniqi S, Matzneller P, Kinzig M, Sörgel F, Hüttner S, Lackner E, et al. Blood, Tissue, and
849 Intracellular Concentrations of Erythromycin and Its Metabolite Anhydroerythromycin during
850 and after Therapy. Antimicrob Agents Chemother. 2012;56: 1059–1064.
851 doi:10.1128/AAC.05490-11

852 48. Somogyi AA, Bochner F, Hetzel D, Williams DB. Evaluation of the Intestinal Absorption of
853 Erythromycin in Man: Absolute Bioavailability and Comparison with Enteric Coated
854 Erythromycin. Pharm Res. 1995;12: 149–154. doi:10.1023/A:1016215510223

855 49. Heldal M, Bratbak G. Production and decay of viruses in aquatic environments. Mar Ecol Prog
856 Ser. 1991;72: 205–212.

857 50. Levin BR, Udekwu KI. Population Dynamics of Antibiotic Treatment: a Mathematical Model and
858 Hypotheses for Time-Kill and Continuous-Culture Experiments. Antimicrob Agents Chemother.
859 2010;54: 3414–3426. doi:10.1128/AAC.00381-10

860 51. Stanczak-Mrozek KI, Laing KG, Lindsay JA. Resistance gene transfer: induction of transducing
861 phage by sub-inhibitory concentrations of antimicrobials is not correlated to induction of lytic
862 phage. J Antimicrob Chemother. 2017;72: 1624–1631. doi:10.1093/jac/dkx056

863 52. Banuelos S, Gulbudak H, Horn MA, Huang Q, Nandi A, Ryu H, et al. Investigating the Impact of
864 Combination Phage and Antibiotic Therapy: A Modeling Study. In: Segal R, Shtylla B, Sindi S,
865 editors. Using Mathematics to Understand Biological Complexity: From Cells to Populations.
866 Cham: Springer International Publishing; 2021. pp. 111–134. doi:10.1007/978-3-030-57129-0_6

867 53. Rodriguez-Gonzalez RA, Leung CY, Chan BK, Turner PE, Weitz JS. Quantitative Models of Phage-
868 Antibiotic Combination Therapy. mSystems. 2020;5: e00756-19. doi:10.1128/mSystems.00756-
869 19

870 54. Liu D, Van Belleghem JD, de Vries CR, Burgener E, Chen Q, Manasherob R, et al. The Safety and
871 Toxicity of Phage Therapy: A Review of Animal and Clinical Studies. Viruses. 2021;13: 1268.
872 doi:10.3390/v13071268

873 55. Imani S, Buscher H, Marriott D, Gentili S, Sandaradura I. Too much of a good thing: a
874 retrospective study of β-lactam concentration–toxicity relationships. J Antimicrob Chemother.
875 2017;72: 2891–2897. doi:10.1093/jac/dkx209

876 56. Koskella B, Brockhurst MA. Bacteria–phage coevolution as a driver of ecological and evolutionary
877 processes in microbial communities. FEMS Microbiol Rev. 2014;38: 916–931. doi:10.1111/1574-
878 6976.12072

879 57. Hampton HG, Watson BNJ, Fineran PC. The arms race between bacteria and their phage foes.
880 Nature. 2020;577: 327–336. doi:10.1038/s41586-019-1894-8

881 58. Dalen R van, Peschel A, Sorge NM van. Wall Teichoic Acid in Staphylococcus aureus Host
882 Interaction. Trends Microbiol. 2020;28: 985–998. doi:10.1016/j.tim.2020.05.017

883